

Propagation failures, breathing pulses, and backfiring in an excitable reaction-diffusion system

Niklas Manz^{a)} and Oliver Steinbock^{b)}

Florida State University, Department of Chemistry and Biochemistry, Tallahassee, Florida 32306-4390

(Received 1 March 2006; accepted 12 July 2006; published online 27 September 2006)

We report results from experiments with a pseudo-one-dimensional Belousov-Zhabotinsky reaction that employs 1,4-cyclohexanedione as its organic substrate. This excitable system shows traveling oxidation pulses and pulse trains that can undergo complex sequences of propagation failures. Moreover, we present examples for (i) breathing pulses that undergo periodic changes in speed and size and (ii) backfiring pulses that near their back repeatedly generate new pulses propagating in opposite direction. © 2006 American Institute of Physics. [DOI: 10.1063/1.2266993]

Chemical reactions far from thermodynamic equilibrium provide simple experimental models for the investigation of self-organization in living organisms. They are ideally suited to test theoretically predicted phenomena that might be present in biological systems but which are inaccessible or obscured by the complexity of the involved processes. A prominent example is the propagation of excitation pulses. This type of structure is crucial for orchestrating the pumping action of the heart and for relaying information in neuronal systems. In the simplest case, excitation pulses have a constant shape and travel steadily through space similarly to a fire spreading through a dry forest. After passage of a refractory period (growth of vegetation), the system locally regains its ability to support new pulses. This feature gives rise to the formation of wave trains and, in two- and three-dimensional media, various types of complex wave patterns such as rotating spirals. Theoretical and numerical studies suggest that excitation pulses can undergo instabilities that induce qualitatively new dynamics. These instabilities induce breathing-like, periodic variations in pulse width and more spectacular behavior in which the pulse emits new pulses near its back. In this paper, we report results obtained from experiments with the well-known Belousov-Zhabotinsky reaction. Our observations provide examples for breathing and backfiring pulses. Moreover, we describe intricate sequences of propagation failures and unexpected variations in pulse duration.

I. INTRODUCTION

Excitable systems show a great variety of propagating wave structures.^{1,2} The underlying pulse trains are not only striking solutions of particular classes of partial differential equations, but they are also found in numerous experimental systems. Prominent examples include concentration waves in chemical reactions³ and propagating action potentials in neuronal systems.⁴ Regardless of the specific nature of the active

medium, relevant models are typically reaction-diffusion (RD) equations and pulses are localized perturbations of finite amplitude. For instance, in the classic Belousov-Zhabotinsky (BZ) reaction,^{5,6} excitation pulses are characterized by a high concentration of bromous acid that is accompanied by a trailing refractory zone in which the reaction's catalyst is being chemically reduced. This refractory zone is not only defining the directionality of pulse propagation, but it also influences the specific velocity of subsequent wavefronts.

The latter dependence is the system-specific dispersion relation $c(\lambda)$, where c is the speed of an infinite wave train with pulse spacing λ . For many experimental systems, the dispersion relation is a monotonically increasing function, which, for large wavelengths, converges to a finite velocity.⁷ This maximal velocity is identical to the speed of the stable solitary pulse. Nonetheless, various theoretical and experimental studies have revealed different types of anomalous dispersion relations. Anomalies include nonmonotonic behavior such as a single overshoot or damped oscillations,^{8,9} bistability,^{10,11} and band gaps.¹² Typically, wave trains exist for every wavelength (or period) above a lower cutoff value. However, recent studies of BZ-type systems showed a peculiar behavior for which wave trains exist only within a finite band of wavelengths. This behavior has been coined "wave tracking."^{13,14} It was also reported for an Oregonator-type model.¹³

Traveling waves of excitation can undergo diverse types of propagation failures. A striking example has been reported for a catalytic surface reaction¹⁵ as well as the 1,4-cyclohexanedione Belousov-Zhabotinsky (CHD-BZ) reaction.^{16,17} This type of behavior affects finite wave packets and is referred to as "wave merging," because fast, trailing pulses vanish periodically in the wake of a slow moving frontier pulse. We note that dispersion relations of CHD-BZ systems with merging and tracking waves have been reported in Refs. 17 and 18, respectively. Moreover, related phenomena also exist in spatially two- and three-dimensional systems.

Wave merging is not the only interesting behavior in the wake of a steadily moving front of excitation. For example,

^{a)}Present address: Henri Begleiter Neurodynamics Laboratory, Department of Psychiatry, SUNY, Downstate Medical Center, 450 Clarkson Avenue, Brooklyn, New York 11203.

^{b)}Electronic mail: steinbock@chem.fsu.edu

traveling fronts can induce stationary, low-amplitude Turing patterns.¹⁹ Also excitation pulses can show a great variety of bifurcations and instabilities. Such instabilities include (i) backfiring pulses that near their back repeatedly start other pulses that travel in opposite direction and (ii) “breathing” pulses that oscillate periodically in shape and speed.^{20–23} Moreover, backfiring (or self-replicating) pulses have attracted considerable interest because the “wave emitting” pulse propagates into a spatially uniform, stable medium and causes complex periodic or spatiotemporal chaotic behavior in its wake.^{20,24}

Both backfiring and breathing can be discussed in terms of traveling wave ordinary differential equations (TWODEs). In this description, pulses are homoclinic orbits and the transitions to backfiring and breathing pulses can be explained as a saddle-node bifurcation and a Hopf instability of the stable pulse solution, respectively. These aspects of pulse bifurcations were discussed in detail for various numerical models such as the Gray-Scott model,²⁵ a model for CO oxidation on Pt(110) (Refs. 21 and 26), as well as the complex Ginzburg-Landau equation.^{27,28}

Despite theoretical interest in pulse bifurcations and instabilities in excitable RD systems, we are aware of only a few experimental systems that show behavior indicating the possible occurrence of the aforementioned pulse instabilities. For instance, Marek *et al.*,^{29,30} and later Sakamoto and Miyakawa,^{31,32} reported complex pulse dynamics for a BZ system in which oxidation and reduction fronts propagate independently at different speeds. In addition, certain morphological patterns in biology could be the result of backfiring pulses such as the intricate patterns on certain mollusk shells.^{33,34} Splitting autowaves were also generated by exposing BZ media to short light pulses³⁵ and electric fields.³⁶ The latter two approaches, however, differ significantly from pulse instabilities in unperturbed media.

Considering the large number of theoretical investigations and the broad diversity of models being analyzed, we see a need for the experimental demonstration of the predicted pulse instabilities and bifurcations. In this paper, we are reporting results obtained from experiments with pseudo-one-dimensional CHD-BZ systems. In particular, we present examples of complex propagation failures, breathing pulses and backfiring pulses.

II. EXPERIMENT

Malonic acid, the classic organic substrate of the BZ system, is replaced by 1,4-cyclohexanedione (CHD). This substitution prevents the formation of detrimental CO₂ bubbles^{37,38} and, more importantly, yields a reaction system with nonmonotonic dispersion relations.^{13,16,17} The redox catalyst is a binary mixture of an iron bathophenanthroline disulphonate complex with either manganous sulfate, cerous sulfate, or ceric sulfate. Fe[batho(SO₃)₂]₃⁴⁻ is used instead of ferroin, because it has a higher absorption contrast between the reduced and oxidized state.³⁹ Stock solutions of 2.0 M NaBrO₃ (Fluka), 0.5 M CHD (Aldrich), 25 mM MnSO₄ (Fisher), 25 mM Ce₂(SO₄)₃ (Aldrich), and 25 mM Ce(SO₄)₂ (Fluka) are prepared in nanopure water (18 MΩ cm) ob-

tained from a Barnstead EASYpure UV unit. The CHD solution is pressed through a Whatman 0.2 μm nylon filter to filter out solid impurities. The 5 M stock solution of H₂SO₄ (Riedel-de Haën) is purchased as standardized solutions and used without further purification. The redox catalyst and indicator Fe[batho(SO₃)₃]₃⁴⁻ (25 mM) is prepared by mixing a 3:1 molar ratio of 4,7-diphenyl-1,10-phenanthroline disulfonic acid disodium salt hydrate (C₂₄H₁₄N₂·2NaO₃S·xH₂O; Acros) with ferrous sulfate heptahydrate (FeSO₄·7H₂O; Fluka) in 25 mM H₂SO₄.

Experiments are carried out in quasi-one-dimensional, thin capillaries with an inner diameter of 0.63 mm and a length of 64 mm (Drummond 20 μl MICROCAPS). The capillary tubes are filled after the reaction solution switches from a spatially homogeneous, oxidized state to a reduced state. This change marks the end of the system's induction time. Depending on the concentrations employed, it occurs 60 to 160 min after starting the reaction by addition of the catalyst solution. If not stated otherwise, the capillaries are placed in a horizontal position. Absorption profiles are monitored with a monochrome charge-coupled-device camera (Uniq UP-2000CL; 1620 × 1236 pixel, 10 bit per pixel). The video signal is digitized using a PC-based frame grabber (R3-PCI-CL13, Bitflow, Inc.). Data are acquired, converted to 8 bit, and saved as bitmap images every 1.0 s using commercial software from Bitflow, Inc. For image analysis we use programs written in IDL (Interactive Data Language, Research System Inc., Versions 5.2). All experiments are performed at (23 ± 1) °C.

III. PROPAGATION FAILURES

In this paper, all halftone figures are space-time plots that comprise the entire photometric data obtained from a given experiment. The space-time plots are generated by sequentially piling up absorption profiles. Accordingly the horizontal and vertical axes are space and time, respectively with time evolving in an upward direction. Bright and dark gray levels correspond to the predominantly oxidized and reduced state of the catalyst, respectively. For experiments that involve mixtures of catalysts, the signals result only from absorption of the iron complex Fe[batho(SO₃)₂]₃^{3-/4-} because for visible light cerium and manganese ions have negligible extinction coefficients.

A typical space-time plot of merging waves is shown in Fig. 1(a). As in all following analyses, each oxidation pulse creates a bright band as it travels through the chemically reduced medium. The speed of the excitation fronts is inversely proportional to the slope of these bands. All pulses nucleate spontaneously at the ends of the capillary tubes. The merging dynamics in Fig. 1(a) reveal a slow leading pulse that is followed by several faster waves. The trailing pulses have a larger width and vanish close to the back of the leading pulse (hence the slightly misleading term “merging”). During their disappearance the pulse width decreases rapidly.

The typical tracking behavior in Fig. 1(c) is similar to the examples published by our group in Refs. 13 and 18. We reemphasize that under these experimental conditions, solitary pulses are unstable and finite wave trains can only ex-

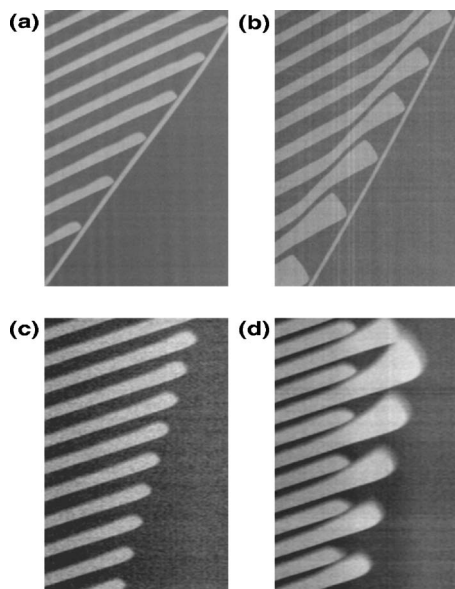


FIG. 1. Space-time plots of wave dynamics in the merging (a), (b) and tracking (c), (d) regime. Examples of simple wave behavior (a), (c) and “trumpet”-like wave ends (b), (d). Initial concentrations: $[\text{H}_2\text{SO}_4]=0.60$ M; $[\text{CHD}]=0.20$ M (a), (c), (d) and 0.22 M (b); $[\text{NaBrO}_3]=0.33$ M (a), 0.34 M (b), 0.32 M (c), and 0.30 M (d); $[\text{Fe}[\text{batho}(\text{SO}_3)_2]_3]=0.10$ mM (a), 0.05 mM (b), and 0.20 mM (c), (d); $[\text{MnSO}_4]=0.40$ mM (a) and 0.45 mM (b); and $[\text{Ce}(\text{SO}_4)_2]=0.30$ mM (c), (d). The horizontal and vertical axes span 15 mm and 500 s (a), (b) and 4.5 mm and 300 s (c), (d), respectively.

pand through repeated propagation failures. In this process each pulse partially “clears the way” for the next pulse which, for sufficiently high frequencies, travels slightly farther than its predecessor. The corresponding dispersion relation is hump-shaped and constrained to a finite band of wavelengths.¹⁸ Analogous behavior is observed in pseudo-two-dimensional media.⁴⁰

While surveying various reaction conditions with mixed catalysts, we discovered that merging and tracking behavior can cause profound variations in pulse width. Figures 1(b) and 1(d) show two typical examples in which pulses increase their width by a factor of up to 4 prior to vanishing. In the space-time plots, this rapid expansion creates the impression of pipe- or trumpetlike structures that differ significantly from the patterns shown in Figs. 1(a) and 1(c).

Further comparison between the space-time plots also reveals interesting differences in the timing of subsequent annihilation events. This observation is most striking in Fig. 1(d) where the propagation failures occur as an alternating sequence of thin and thick pulses. Furthermore, the thin pulses vanish within the pulse train while the trumpetlike, inflated pulses disappear at the boundary of the wave train. Consequently, only the trumpetlike waves drive the expansion of the pattern.

Figure 2 provides additional examples for the great variety of shapes and rhythms that are associated with these intriguing dynamics. The example in Fig. 2(a) shows merging waves, while Figs. 2(b)–2(d) are obtained for tracking conditions. In all four cases, we find intricate and repeating sequences of short, narrow and long, wide pulses. For instance, Fig. 2(c) shows a firing pattern that can be described as repeating blocks of long, very long, short, medium, and

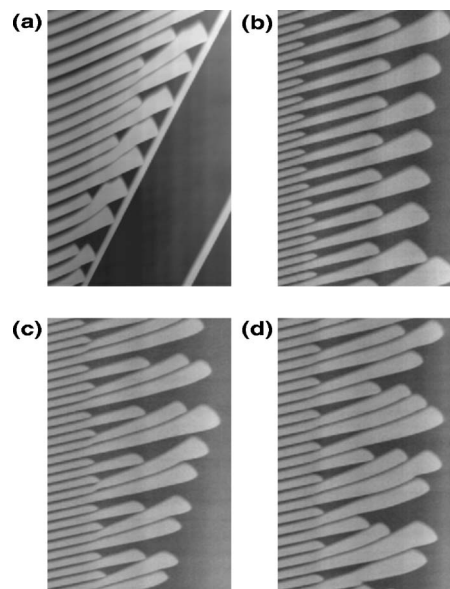


FIG. 2. Space-time plots of complex wave dynamics in the merging (a) and tracking regime (b)–(d). Initial concentrations: $[\text{H}_2\text{SO}_4]=0.60$ M, $[\text{CHD}]=0.20$ M, $[\text{NaBrO}_3]=0.27$ M (a) and 0.30 M (b)–(d), $[\text{Fe}[\text{batho}(\text{SO}_3)_2]_3]=0.40$ mM (a) and 0.10 mM (b)–(d), $[\text{Ce}_2(\text{SO}_4)_3]=0.10$ mM (a), and $[\text{Ce}(\text{SO}_4)_2]=0.40$ mM (b)–(d). The horizontal and vertical axes span 14.7 mm and 600 s (a), (b) and 6.3 mm and 700 s (c), (d), respectively.

short pulses. None of these complex patterns is stable over long times, which is probably due to (a) a mild parameter drift caused by the slow consumption of chemical reactants and (b) the high density of different firing sequences in the system’s parameter space. It appears likely that a drift-free medium would reveal a scenario that is similar to devil’s staircases which exist in a variety of systems ranging from Cantor sets⁴¹ to quantized spiral tip motion in heterogeneous excitable systems.³⁹

IV. BREATHING PULSES

Figure 3 shows space-time plots that exemplify a qualitatively novel type of pulse propagation. In both experiments, the leading pulses have a constant shape and velocity. Most of the trailing pulses, however, reveal oscillatory changes in their width and speed. These changes occur around mean values that are very similar or identical to the constant width and speed of the leading pulse. The typical oscillation period is 22 s. The oscillating or breathing pulses are susceptible to propagation failures. Typically the pulses vanish in the oscillation phase for which one would expect a small or minimal width. Moreover, the leading, oxidation side of the breathing pulses shows slightly larger variation in speed than the trailing wake where the pulse switches back into the chemically reduced state. Our observations indicate that these velocity changes can be quite pronounced. For instance, we find minimal and maximal front speeds of 25 and 50 $\mu\text{m/s}$ for the fifth pulse in Fig. 3(a).

Both experiments shown in Fig. 3 employ a mixture of manganese ion and iron complex as their catalyst. The mole ratio of the two species is $\text{Mn}:\text{Fe}=30:1$. We suggest that under these conditions the system dynamics is determined by the kinetics of manganese ion while the iron complex merely

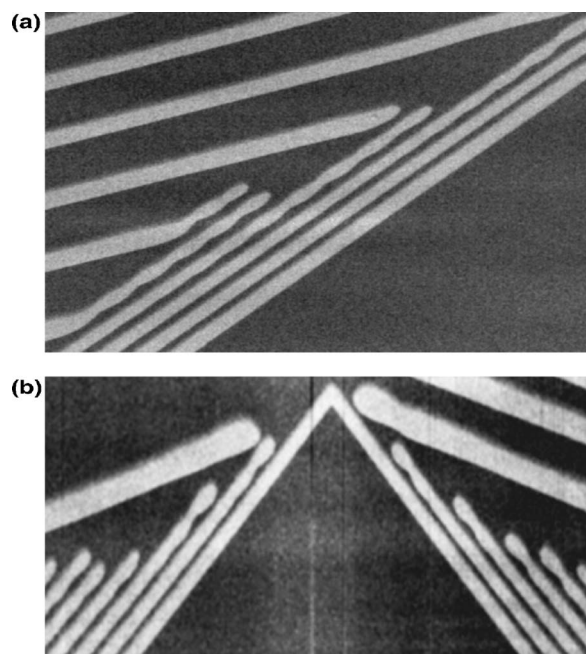


FIG. 3. Space-time plots of wave dynamics with breathing pulses in a horizontal (a) and a vertical (b) CHD-BZ system. Waves moving to the right (left) in (b) propagate upwards (downwards) in the capillary. Initial concentrations: $[\text{H}_2\text{SO}_4]=0.60$ M, $[\text{CHD}]=0.23$ M (a) and 0.22 M (b), $[\text{NaBrO}_3]=0.33$ M (a) and 0.32 M (b), $[\text{Fe}[\text{batho}(\text{SO}_3)_2]_3]=0.05$ mM, and $[\text{MnSO}_4]=1.5$ mM. The horizontal and vertical axes span 11.1 mm and 300 s (a) and 17.1 mm and 250 s (b), respectively.

serves as a redox indicator. Moreover, we note that the large iron complex (molar mass 1527 g/mol) has a significantly smaller diffusion constant than the small manganese ion. Consequently, we expect that all dynamically relevant species in the experiments (Fig. 3) have essentially identical diffusion constants.

One potential concern regarding the occurrence of breathing and other oscillatory wave structures is the possible presence of fluid convection. Hydrodynamic flow cells within the capillary tube could be induced by the mild exothermicity of the reaction. To rule out this conceivable source of breathing dynamics, we compared the wave behavior in capillaries with inner diameters of $(0.20\text{--}0.80)$ mm but found no dependence of the breathing period on the capillary diameter. Moreover, we did not find any systematic differences between vertical and horizontal reaction systems. The latter finding is also illustrated in Fig. 3 where the two plots are obtained from experiments with a horizontal (a) and a vertical capillary (b).

The breathing pulses observed here are likely to arise from a pulse instability that had been predicted in earlier theoretical and numerical investigations. In these studies the breathing motion occurs via a supercritical Hopf bifurcation of the steadily traveling wave. The resulting pulses are also referred to as “modulated traveling pulses”²⁰ or “wobbling waves.”⁴² Furthermore, theoretical analyses reveal additional bifurcations to period-2, period-4, and chaotic behavior.²⁰ Our experiments, however, seem to obey simple periodic motion, which obviously does not rule out the existence of more complex behavior for other sets of initial concentra-

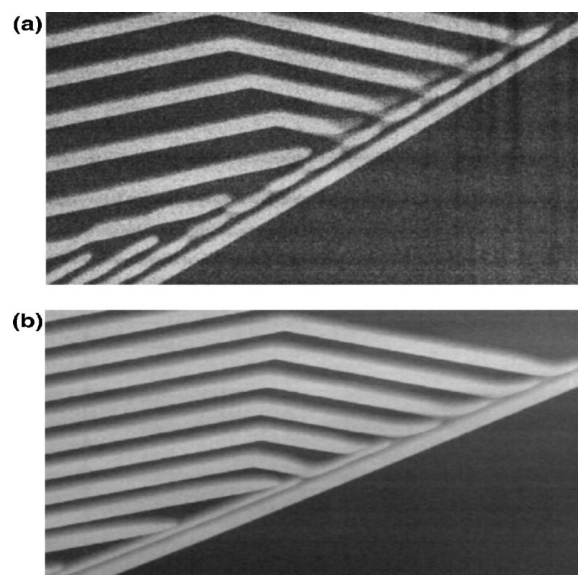


FIG. 4. Examples of backfiring in the CHD-BZ reaction. Initial concentrations: $[\text{H}_2\text{SO}_4]=0.60$ M, $[\text{CHD}]=0.22$ M (a) and 0.20 M (b), $[\text{NaBrO}_3]=0.32$ M (a) and 0.33 M (b), $[\text{Fe}[\text{batho}(\text{SO}_3)_2]_3]=0.05$ mM (a) and 0.25 mM (b), $[\text{MnSO}_4]=1.5$ mM (a), and $[\text{Ce}(\text{SO}_4)_2]=0.25$ mM (b). The horizontal and vertical axes span 11 mm and 300 s, respectively.

tions. Moreover, it is not clear why only closely spaced waves undergo the breathing motion while widely spaced pulses appear to maintain a constant width and speed.

V. BACKFIRING PULSES

Backfiring or wave-emitting pulses are another interesting case of wave dynamics in one-dimensional excitable systems. This behavior has been predicted by several theoretical studies which, as discussed in the Introduction, identify the underlying pulse bifurcation as a saddle-node bifurcation. We note that backfiring might also be induced by other bifurcations, such as pitchfork and transcritical bifurcations, although the latter cases require particular symmetries in models and solutions. Furthermore, the term pulse is used only loosely in this context since the wave-emitting behavior is characteristic and intrinsic to the coherent traveling structure.

Figure 4 shows two examples of backfiring pulses. In both cases, the backfiring structure is the pulslike object trailing in the wake of the leading pulse. While the leading and the backfiring pulses travel rightward, all emitted pulses move leftward. The backfiring periods are 36 and 31 s in (a) and (b), respectively. The newly emitted pulses form a wave train that collides with other incoming pulses. Due to the specific differences in the periods of these wave trains, we observe a leftward shifting collision line in Fig. 4(a) and a rightward moving collision line in Fig. 4(b).

The backfiring pulses in Fig. 4 are observed in CHD-BZ systems with mixed catalysts. More specifically, the two examples employ mixtures of manganese ion and iron complex in (a) and cerium ion and iron complex in (b). The mole ratios are $\text{Mn}:\text{Fe}=30:1$ and $\text{Ce}:\text{Fe}=1:1$, respectively. Since the latter ratio equals one, we expect that both catalyst species are relevant for the observed dynamics. Moreover, we

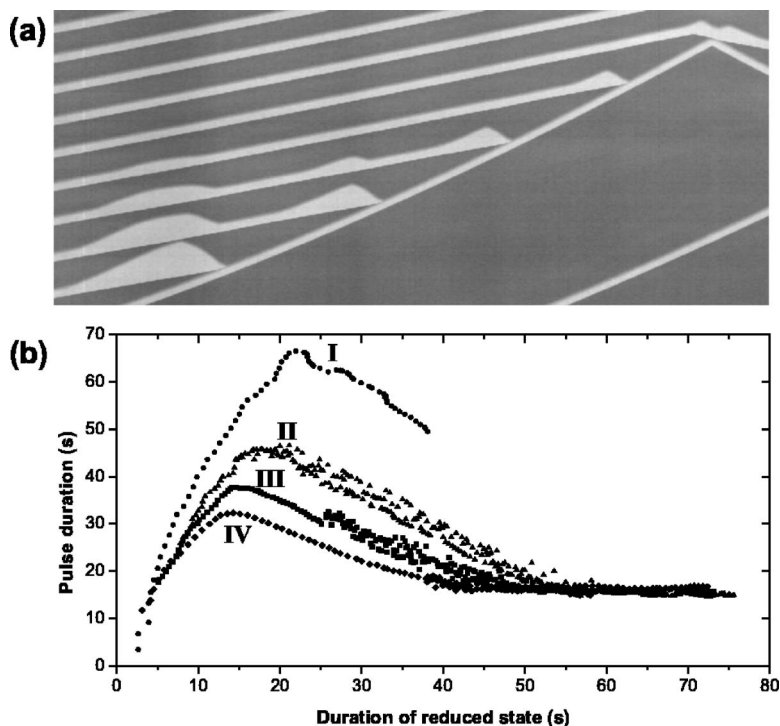


FIG. 5. (a) Space-time plot of echo-like changes in pulse duration for merging waves. The horizontal and vertical axes span 25 mm and 600 s, respectively. (b) Dependence of the pulse duration on the duration of the preceding reduced state. The Roman numerals I to IV denote subsequent trailing pulses in (a). Initial concentrations: $[\text{H}_2\text{SO}_4]=0.60$ M, $[\text{CHD}]=0.20$ M, $[\text{NaBrO}_3]=0.32$ M, $[\text{Fe}[\text{batho}(\text{SO}_3)_2]_3]=0.20$ mM, and $[\text{Ce}(\text{SO}_4)_2]=0.30$ mM.

did not observe any indications for backfiring pulses in CHD-BZ systems with pure ferroin ($\text{Fe}(\text{phen})_3$) or $\text{Fe}[\text{batho}(\text{SO}_3)_2]_3$ catalysts, although the Ce:Fe ratio is much smaller than the Mn:Fe ratio.

Closer inspection of the backfiring pulses in Fig. 4 reveals that the wave-emitting structures are segmented. This finding is more pronounced in Fig. 4(a) where each segment corresponds to one pulse emission event. Furthermore, the latter experiment shows an initial breathing motion of the second pulse that then changes into the wave-emitting state.

Lastly, we reemphasize that the observed dynamics in the wake of our backfiring pulses is simple periodic in time. Although we cannot rule out more complex behavior for larger systems and longer lifetimes, the observations clearly differ from spatio-temporally chaotic behavior that can be associated with backfiring pulses. In particular, we do not observe backfiring of pulses that themselves were created in backfiring events.

VI. LONG-LIVED OXIDATION STATES

While the observed breathing and backfiring pulses are likely to exemplify instabilities that have been predicted for one-dimensional excitable media, we also find more unexpected dynamics. Figure 5(a) shows a space-time plot of several rightward propagation pulses in a Ce/Fe catalyzed CHD-BZ system. The overall dynamics of this system can be summarized as “merging” where fast trailing pulses vanish near the back of a slowly moving frontier pulse. The space-time plot shows two near solitary pulses (i.e., large distance to predecessors). The second pulse is followed by several fast waves. The first four of these trailing pulses show unusual variations in pulse width. These variations do not affect the speed of the pulses’ oxidation fronts but only increase the lifetime of the oxidation state. Furthermore, these variations

can occur several times for a given pulse. They are triggered by the preannihilation broadening of the pulse itself or the preannihilation broadening of one of its predecessors as the initial perturbation locally affects several trailing pulses in an echo-like fashion.

The phenomenon of pulse broadening is analyzed in Fig. 5(b). The plot shows the duration of the oxidized state as a function of the duration of the preceding reduced state. The analysis is carried out for the trailing pulses that show detectable changes in pulse width. The data from these four waves are distinguished by different symbols and Roman numerals. The Roman numeral “I” denotes the first trailing pulse in Fig. 5(a). All four data sets approach a pulse duration of approximately 16 s for reduction times larger than 50 s. For shorter reduced states the pulse duration increases to values of more than 60 s. This increase, however, is most pronounced for the pulse “I” and decreases for the subsequent pulses “II”–“IV.” The shortest pulse durations correspond to near-annihilation states. The overall data are reminiscent of the system’s anomalous dispersion relation, but it is unclear why the velocity of oxidation fronts does not change at all. Furthermore, it is surprising that the velocity of the reduction front causes the observed variation in pulse duration and responds sensitively to the preceding reduction event. Consequently, the observed dynamics are clearly different from the observed breathing behavior (cf. Fig. 4).

Many of our observations indicate that the oxidized state can have unusually long lifetimes, but this state does not appear to be a stable fixed point. Figure 6 shows a space-time plot revealing complex behavior in the wake of stable, slow oxidation pulses. In this example, waves are entering the field of view from both sides. Trailing, fast pulses are annihilating near the back of their slower counterparts. This annihilation is preceded by an increase in pulse duration

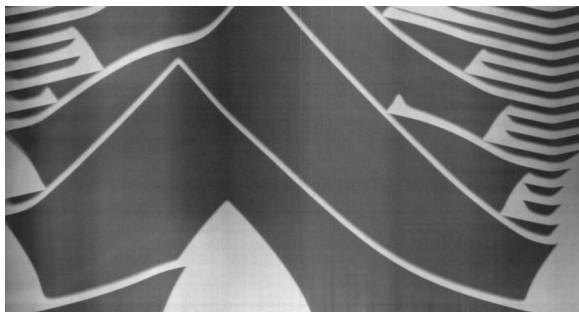


FIG. 6. Complex wave behavior in the CHD-BZ reaction. Initial concentrations: $[\text{H}_2\text{SO}_4]=0.60\text{ M}$, $[\text{CHD}]=0.20\text{ M}$, $[\text{NaBrO}_3]=0.30\text{ M}$, $[\text{Fe}(\text{batho}(\text{SO}_3)_2)_3]=0.25\text{ mM}$, and $[\text{Ce}(\text{SO}_4)_2]=0.25\text{ mM}$. The horizontal and vertical axes span 34 mm and 860 s, respectively.

similar to the behavior discussed in the context of Figs. 2 and 5. Subsequent pulses, however, tend to merge into the trumpetlike regions causing locally long-lived oxidation states. This merging of pulses leads to a coherent structure that retreats via a reversely traveling reduction front. The speed of these reduction fronts is similar to the typical speed of the dominant oxidation transitions.

VII. CONCLUSIONS

In conclusion, this paper has presented experimental evidence for pulse instabilities that were predicted in earlier theoretical studies but, to our knowledge, had not yet been observed in a chemical system. These instabilities give rise to breathing and backfiring pulses. Both phenomena introduce a characteristic periodicity in the one-dimensional reaction system without relying on a Hopf bifurcation of the spatially homogeneous medium. Moreover, we have presented unusual and unexpected features of propagation failures that give rise to intricate rhythms reminiscent of firing numbers in temporal systems. These propagation failures also profoundly alter pulse shapes. This finding is unusual because typical BZ systems show little variation in pulse duration. Moreover, it appears that the back of the oxidation pulse can decouple from the motion of the oxidation front, thus, causing a wealth of complex wave patterns.

Up to now, we have observed breathing and backfiring pulses only in Ce/Fe and Mn/Fe catalyzed CHD-BZ systems. Despite thorough exploration of the $\text{Fe}(\text{phen})_3$ -CHD-BZ parameter space and many experiments with the $\text{Fe}(\text{batho}(\text{SO}_3)_2)_3$ -CHD-BZ reaction, we did not find these instabilities in any, strictly iron-complex catalyzed system. The redox catalysts employed in this study differ in redox potential, kinetics, and diffusion constants. In contrast to $\text{Fe}(\text{batho}(\text{SO}_3)_2)_3$ and $\text{Fe}(\text{phen})_3$, the diffusion constants of the small cerium and manganese ions are comparable to those of the activator HBrO_2 and the inhibitor Br^- . This similarity of manganese and cerium ion suggests that the ratio of diffusion constants is an important factor. Specifically, one can hypothesize that breathing and backfiring pulses occur only in CHD-BZ systems where the key species have equal or similar diffusion constants. Additional measurements and

a detailed characterization of the underlying phase diagrams are needed to provide more definite insights into the importance of the catalyst species.

For future experimental studies, it will be also interesting to explore the effects of breathing and backfiring pulses on two-dimensional wave patterns such as rotating spiral waves. In particular, it appears likely that the CHD-BZ reaction can be used for the experimental investigation of particular spiral breakup scenarios. The latter behaviors have attracted considerable interest because they could be a major factor in the dynamics of cardiac arrhythmia.⁴³

ACKNOWLEDGMENT

This work was supported by the Chemistry Division of the National Science Foundation (Grant No. CHE-0513912). N.M. thanks the “Deutsche Akademie für Naturforscher Leopoldina” (Grant No. BMBF-LPD 9901/8-85) for financial support. We thank Brent T. Ginn for discussions.

¹M. C. Cross and P. C. Hohenberg, “Pattern formation outside of equilibrium,” *Rev. Mod. Phys.* **65**, 851–1112 (1993).

²*Spatio-Temporal Pattern Formation (With Examples from Physics, Chemistry, and Materials Science)*, edited by C. Walgraef (Springer Verlag, New York, 1997).

³*Chemical Waves and Patterns*, edited by R. Kapral and K. Showalter (Kluwer, Dordrecht, The Netherlands, 1995).

⁴H. Zhang and A. V. Holden, “Defibrillation threshold computed from normal and supernormal excitable cardiac tissue,” *Math. Biosci.* **188**, 175–190 (2004).

⁵A. M. Zhabotinsky, “Periodic Processes of the Oxidation of Malonic Acid in Solution (Investigation of the Kinetics of the Reaction of Belousov),” *Biophysics (Engl. Transl.)* **9**, 329–335 (1964); *Biofizika* **9**, 306–311 (1964).

⁶A. N. Zaikin and A. M. Zhabotinsky, “Concentration wave propagation in two-dimensional liquid-phase self-oscillating system,” *Nature (London)* **225**, 535–537 (1970).

⁷J.-M. Flesselles, A. Belmonte, and V. Gáspár, “Dispersion relation for waves in the Belousov-Zhabotinsky reaction,” *J. Chem. Soc., Faraday Trans.* **94**, 851–855 (1998).

⁸C. Elphick, E. Meron, and E. A. Spiegel, “Spatiotemporal complexity in traveling patterns,” *Phys. Rev. Lett.* **61**, 496–499 (1988).

⁹C. Elphick, E. Meron, J. Rinzel, and E. A. Spiegel, “Impulse patterning and relaxational propagation in excitable media,” *J. Theor. Biol.* **146**, 249–268 (1990).

¹⁰G. Bordiougov and H. Engel, “Oscillatory dispersion and coexisting stable pulse trains in an excitable medium,” *Phys. Rev. Lett.* **90**, 148302 (2003).

¹¹G. Bordiougov and H. Engel, “From trigger to phase waves and back again,” *Physica D* **215**, 25–37 (2006).

¹²M. Falcke, M. Or-Guil, and M. Bär, “Dispersion gap and localized spiral waves in a model for intracellular Ca^{2+} dynamics,” *Phys. Rev. Lett.* **84**, 4753–4756 (2000).

¹³N. Manz, C. T. Hamik, and O. Steinbock, “Tracking waves and vortex nucleation in excitable systems with anomalous dispersion,” *Phys. Rev. Lett.* **92**, 248301 (2004).

¹⁴N. Manz and O. Steinbock, “Tracking waves and spiral drift in reaction-diffusion systems with finite bandwidth dispersion relations,” *J. Phys. Chem.* **108**, 5295–5298 (2004).

¹⁵J. Christoph, M. Eiswirth, N. Hartmann, R. Imbühl, I. G. Kevrekidis, and M. Bär, “Anomalous dispersion and pulse interaction in an excitable surface reaction,” *Phys. Rev. Lett.* **82**, 1586–1589 (1999).

¹⁶N. Manz, S. C. Müller, and O. Steinbock, “Anomalous dispersion of chemical waves in a homogeneously catalyzed reaction system,” *J. Phys. Chem. A* **104**, 5895–5896 (2000).

¹⁷C. T. Hamik, N. Manz, and O. Steinbock, “Anomalous dispersion and attractive pulse interaction in the 1,4-cyclohexanedione Belousov-Zhabotinsky reaction,” *J. Phys. Chem. A* **105**, 6144–6153 (2001).

¹⁸N. Manz, B. T. Ginn, and O. Steinbock, “Propagation failure dynamics of wave trains in excitable systems,” *Phys. Rev. E* **73**, 066218 (2006).

¹⁹B. Sandstede and A. Scheel, “Spectral stability of modulated travelling

- waves bifurcating near essential instabilities," *Proc. - R. Soc. Edinburgh, Sect. A: Math.* **130**, 419–448 (2000).
- ²⁰J. Krishnan, I. G. Kevrekidis, M. Or-Guil, M. Zimmermann, and M. Bär, "Numerical bifurcation and stability analysis of solitary pulses in an excitable reaction-diffusion medium," *Comput. Methods Appl. Mech. Eng.* **170**, 253–275 (1999).
- ²¹M. Or-Guil, J. Krishnan, I. G. Kevrekidis, and M. Bär, "Pulse bifurcations and instabilities in an excitable medium: Computations in finite ring domains," *Phys. Rev. E* **64**, 046212 (2001).
- ²²M. Courtémanche, L. Glass, and J. P. Keener, "A delay equation representation of pulse circulation on a ring in excitable media," *SIAM J. Appl. Math.* **56**, 119–142 (1996).
- ²³V. B. Kazantsev, V. I. Nekortin, S. Binczak, and J. M. Bilbault, "Spiking patterns emerging from wave instabilities in a one-dimensional neural lattice," *Phys. Rev. E* **68**, 017201 (2003).
- ²⁴Y. Hayase and T. Ohta, "Self-replicating pulses and Sierpinski gaskets in excitable media," *Phys. Rev. E* **62**, 5998–6003 (2000).
- ²⁵Y. Nishiura and D. Ueyama, "A skeleton structure of self-replicating dynamics," *Physica D* **130**, 73–104 (1999).
- ²⁶M. Bär, M. Hildebrand, M. Eiswirth, M. Falcke, H. Engel, and M. Neufeld, "Chemical turbulence and standing waves in a surface reaction model: The influence of global coupling and wave instabilities," *Chaos* **4**, 499–508 (1994).
- ²⁷L. Brusch, M. G. Zimmermann, M. van Hecke, M. Bär, and A. Torcini, "Modulated amplitude waves and the transition from phase to defect chaos," *Phys. Rev. Lett.* **85**, 86–89 (2000).
- ²⁸M. Argentina, O. Rudzick, and M. G. Velarde, "On the backfiring instability," *Chaos* **14**, 777–783 (2004).
- ²⁹M. Marek, P. Kaštník, and S. C. Müller, "Ring-shaped waves of inhibition in the Belousov-Zhabotinsky reaction," *J. Phys. Chem.* **98**, 7452–7454 (1994).
- ³⁰P. Kaštník, J. Kosek, D. Šnita, I. Schreiber, and M. Marek, "Reduction waves in the BZ reaction: Circles, spirals and effects of electric field," *Physica D* **84**, 79–94 (1995).
- ³¹F. Sakamoto and K. Miyakawa, "Self-replication and preservation of reduction waves in the Belousov-Zhabotinsky reaction," *J. Phys. Soc. Jpn.* **69**, 2775–2778 (2000).
- ³²F. Sakamoto and K. Miyakawa, "Asymmetric spatiotemporal patterns of reduction waves in the Belousov-Zhabotinsky reaction," *J. Phys. Soc. Jpn.* **70**, 2263–2266 (2001).
- ³³H. Meinhardt and M. Klingler, "A model for pattern formation on the shells of molluscs," *J. Theor. Biol.* **126**, 63–89 (1987).
- ³⁴*Mathematical Biology*, edited by J. D. Murray, 3rd ed. (Springer-Verlag, Berlin, 2002).
- ³⁵A. P. Muñuzuri, V. Pérez-Villar, and M. Markus, "Splitting of autowaves in an active medium," *Phys. Rev. Lett.* **79**, 1941–1944 (1997).
- ³⁶H. Ševčíková, J. Kosek, and M. Marek, "Splitting of 2D waves of excitation in a direct current electric field," *J. Phys. Chem.* **100**, 1666–1675 (1996).
- ³⁷K. Kurin-Csörgei, I. Szalai, I. Molnár-Perl, and E. Körös, "The 1,4-cyclohexanedione-bromat-acid oscillatory system, I: Its organic chemistry," *React. Kinet. Catal. Lett.* **53**, 115–121 (1994).
- ³⁸K. Kurin-Csörgei, I. Szalai, and E. Körös, "The 1,4-cyclohexanedione-bromat-acid oscillatory system, II: Chemical waves," *React. Kinet. Catal. Lett.* **54**, 217–224 (1995).
- ³⁹B. T. Ginn, B. Steinbock, M. Kahveci, and O. Steinbock, "Microfluidic systems for the Belousov-Zhabotinsky reaction," *J. Phys. Chem. A* **108**, 1325–1332 (2004).
- ⁴⁰N. Manz, B. T. Ginn, and O. Steinbock, "Meandering spiral waves in the 1,4-cyclohexanedione Belousov-Zhabotinsky system catalyzed by $\text{Fe}[\text{batho}(\text{SO}_3)_2]_3^{4-/3-}$," *J. Phys. Chem. A* **107**, 11008–11012 (2003).
- ⁴¹*Fractals, Chaos, Power Laws*, M. Schroeder (Freeman, New York, 1991).
- ⁴²H. S. Brown and I. G. Kevrekidis, "Modulated travelling waves in the Kuramoto-Sivashinsky equation," *Fields Inst. Commun.* **5**, 45–66 (1996).
- ⁴³A. Karma, "Spiral breakup in model equations of action potential propagation in cardiac tissue," *Phys. Rev. Lett.* **71**, 1103–1106 (1993).